Received: 13 October 2021 | Revised: 30 November 2021 | Accepted: 15 January 2022

DOI: 10.1002/asl.1084

RESEARCH ARTICLE

Atmospheric Science Letters RMetS

On gravity wave parameterisation in vicinity of low-level blocking

Markus Geldenhuys[1,2]

[1]Stratosphere 4 (IEK-7), Forschungszentrum Juelich, Institute of Energy and Climate Research, Juelich, Germany

[2]South African Weather Service, Pretoria, South Africa

Correspondence
Markus Geldenhuys, Stratosphere 4 (IEK-7), Forschungszentrum Juelich, Institute of Energy- and Climate Research, Juelich 52428, Germany.
Email: markusgeld@gmail.com

Abstract

This note is framed as an open question to the community regarding parameterisation schemes using the blocking layer depth to reduce the orographic gravity wave drag. It is the purpose of this note to argue that the current orographic gravity wave drag parameterisation in the vicinity of blocking is inadequate. Reducing the gravity wave amplitude (and thereby reducing the gravity wave drag) by assuming an effective mountain height dependent on the blocking depth is not realistic. The arguments given here will hopefully spark a debate and new considerations, ultimately leading to improvements in current orographic gravity wave drag parameterisations. This note illustrates that low-level blocking can induce more gravity waves or gravity waves with a higher momentum flux (compared to the current parameterisation schemes). More realistic parameterisation schemes are likely to improve the models' performance. However, the fact is complex theories are needed to describe gravity wave excitation by orography so that it is difficult to represent gravity wave nature by a 'too simple' parameterisation scheme.

KEYWORDS

blocking, drag, gravity wave, mountain wave, parameterisation

1 | INTRODUCTION

The parameterised part of the gravity wave (GW) spectrum is ever-shrinking with increases in computational power. However, Berner et al. (2017) suggest that in future computational resources can likely be directed to running more ensemble members or running an Earth system model. Recently Lang et al. (2021) doubled the operational Integrated Forecast System (IFS) vertical resolution and still the model required parameterisation schemes. This means at the highest feasible resolution the whole GW spectrum is far from being resolved. With these trends and the restriction on computational growth in mind, parameterisation schemes are expected to be around for some time to come. Correct parameterisations are required to represent real-world dynamics which the model cannot resolve.

Gravity waves are important for the dynamics in the atmosphere (Fritts & Alexander, 2003; Sato & Hirano, 2019). It is well known that to have a respected and accurate model, GW drag needs to be represented realistically. However, Sandu et al. (2016) found models differ by as much as 20% in their surface sub-grid stress. To represent reality, GW parameterisation schemes are required to represent GWs not explicitly resolved in the model. Every model is different concerning the amount of drag produced. Some models adjust the GW drag by looking at

basic variables, and others have a 'knob' in their equations which can be used to increase or decrease the drag (Kim & Doyle, 2005; Polichtchouk et al., 2018; Sandu et al., 2016). This reveals the uncertainty and lack of physical realism in these schemes.

Recently Plougonven et al. (2020) highlighted the remaining unaccounted GW phenomena in parameterisation schemes; secondary emission, lateral propagation and transience. The community is actively addressing these issues. For example, a new transient GW parameterisation scheme is currently being developed (Boeloeni et al., 2021; Kim et al., 2021), and the BMBF WASCLIM ROMIC II project develops a mountain wave (MW) model to help address lateral propagation (based on Bacmeister et al., 1994). Recently, Van Niekerk and Vosper (2021) implemented a 'scale-aware' orographic GW drag scheme that represents the whole sub-grid GW spectrum. Many other studies exist with constant improvements being made in GW parameterisation schemes (de la Camara et al., 2016; Garcia et al., 2017; Lott et al., 2012; McLandress et al., 2012; Plougonven et al., 2020; Polichtchouk et al., 2018; Xie et al., 2019). Currently, an ISSI Team exists focusing only on identifying constraints on orographic GW drag (http://www.issibern.ch/teams/consonorogravity). Even observational campaigns have dedicated objectives to improve understanding of GWs for improvement of parameterisation schemes (Fritts et al., 2016; Rapp et al., 2021; Serafin et al., 2020). The amount of ongoing work in the community is indeed refreshing. This note does not intend to address any of the above issues, but instead hints at a new one.

Wind flow is blocked by a mountain barrier if it does not have enough momentum to ascend the barrier. Blocking is found in all mountainous areas, as long as the stability and wind requirements are met (Smith, 2019). Blocking takes place when cold stable air does not have sufficient momentum to pass over a barrier and is deflected (Geldenhuys et al., 2019; Neiman et al., 2010; Smith, 2019). Locally, this results in a higher pressure with an increase in the pressure gradient and in turn a stronger wind. The mountain deflects the wind and a low-level wind is formed parallel to the mountain barrier. This stronger (and deflected) wind is called the blocking jet (although it is called a jet it merely acts as a reference to the stronger wind). This low-level jet is characterised by a higher pressure, stronger winds and a deflected wind direction. This jet continues to build upwind and has been observed to extend up to 200 km upwind of the barrier (Loescher et al., 2006).

Most MW parameterisation schemes (Kim & Arakawa, 1995; Kim & Doyle, 2005; Lott & Miller, 1997; Pierrehumbert, 1986; Sandu et al., 2016; Xie et al., 2019) have the GW drag dependent by some means on low-level blocking. Schemes building on Pierrehumbert (1986) (Kim & Arakawa, 1995; Kim & Doyle, 2005; Xie et al., 2019) scale the GW drag at reference level with the wind projected onto the low-level wind direction (the blocking wind direction). In a typical blocking case, the wind direction at low levels and the reference level (above the terrain) can differ anything from a few degrees to $\approx 90^{\circ}$. This means that the wind entering the GW drag, Equation (1) (eq. 6 from Kim & Doyle, 2005) can be reduced drastically, reducing the resultant GW drag. To illustrate the maximum reduction, a blocking case from Geldenhuys et al. (2019) is represented in Figure 1d. If the wind at reference level (dashed arrow) is projected to the blocking jet direction the wind speed would reduce to ≈ 0

$$\tau_{\mathrm{GWD}} = \rho_0 E \frac{m}{\lambda_{\mathrm{eff}}} G \frac{|U_0|^3}{N_0}, \tag{1}$$

where τ_{GWD} is the calculated GW drag, ρ_0 is density, E is an enhancement factor, m is the number of mountains, λ_{eff} is the grid length or acts as a tuning coefficient, G is an asymptotic function to facilitate a smooth transition between 2D blocking and non-blocking cases, U_0 is horizontal wind speed at reference level that is projected onto the low-level wind direction (blocking jet) and N_0 is the low-level Brünt–Väisälä frequency. For an in-depth explanation of the formula and its terms, refer to Kim and Doyle (2005).

In schemes building on Lott and Miller (1997) (e.g., the European Centre for Medium-Range Weather Forecasts (ECMWF), see Sandu et al., 2016), the GW drag is reduced exponentially depending on the blocking layer depth (eqs. 2 and 3 from ECMWF, 2015). ECMWF employ

$$\tau_{\mathrm{GWD}} = \rho_0 b G_s B(\gamma) \mathrm{NUH}^2_{\mathrm{eff}}, \tag{2}$$

where b is the mountain height variation in the along-ridge direction, G_s is a function of mountain sharpness, γ represents mountain anisotropy and B is a function of γ which can vary from 1 for a 2D ridge and $\pi/4$ for a circular mountain. H_{eff} is the effective mountain height represented by

$$H_{\mathrm{eff}} = 2(H - Z_{\mathrm{blk}}), \tag{3}$$

where H is the ridge height and Z_{blk} is the depth of the blocking layer. Equation 3 shows that the GWD depends exponentially on the blocking layer depth. The models assume that with an increase in the blocking layer depth, the layer of wind approaching the terrain is reduced, and the GW field is reduced (Figure 1b as opposed to the normal case of Figure 1a). Many idealised 2D models also follow this approach and reduce the GW field depending

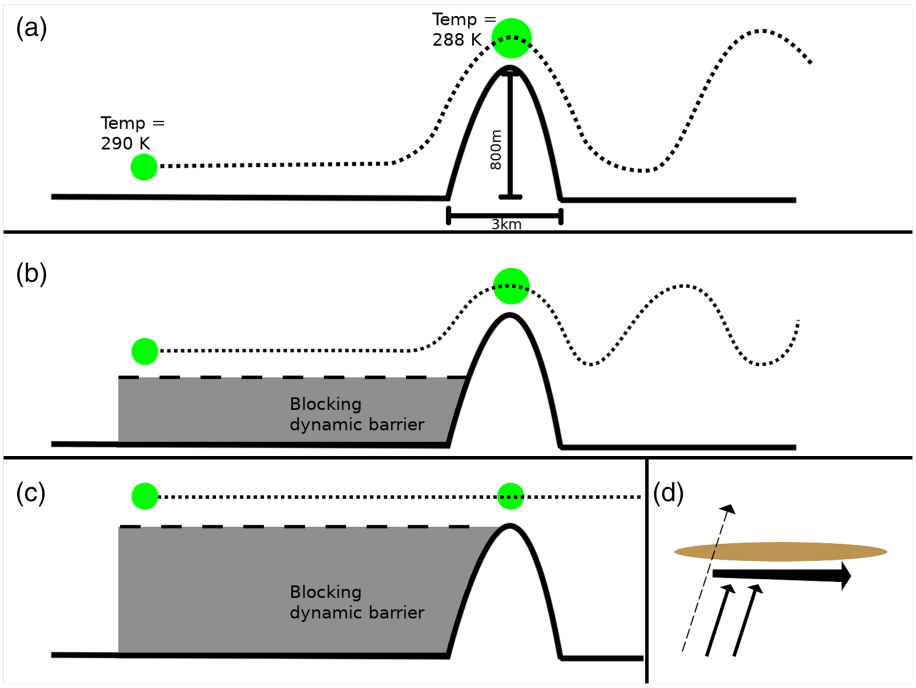

FIGURE 1 Mountain waves as assumed by the model parameterisation schemes. Mountain dimensions are based on the case by Geldenhuys et al. (2019), but can take any values. Green circles indicate the air parcels being uplifted and dotted lines indicate the wind perpendicular to the mountain ridge. Panel (a) shows the typical MW formation. Panels (b) and (c) show what the model assumes different stages of blocking (shaded part) and what its corresponding MW look like. Note that Panel (c) represents a complete blocking layer up to mountain height. Here, the model perceives no vertical displacement, thus producing no GW drag. Panel (d) shows the blocking situation from above. The large arrow represents the blocking jet (dynamic barrier) the solid arrows represent the incoming low-level winds and the dashed arrow indicates the wind ≈ 500 m above the terrain. In Equation (1), the dashed arrow projected onto the large arrow form U_0. The figure is not to scale

on the depth of the wind approaching the barrier. This assumption reduces the amplitude of the GW (it is important to take note of this, as the rest of this note will frequently refer to this reduction). This means that the assumed (by the models who have some variant of this configuration) GW depends only on the wind from the blocking layer top to the mountain top. Although this is based on semi-sound principles, I argue this can cause the model to underestimate GW drag. In the following sections of this note, I suggest that a more realistic approach would be if parameterisation schemes account less for the blocking layer in GW generation.

2 | WHY DO PARAMETERISATION SCHEMES ACCOUNT FOR THE BLOCKING LAYER IN DETERMINING GW DRAG?

Compared to the environmental conditions, the blocking region is characterised by a higher pressure, stronger wind and a deflected wind direction (Geldenhuys et al., 2019; Neiman et al., 2010; Smith, 2019). This blocking region with different characteristics forms a dynamic barrier (Geldenhuys et al., 2019; Neiman et al., 2010). The dynamic barrier takes a variety of different names in literature, for example Bell and Bossart (1988) refer to it as a cold dome with a low-level wind maximum while it is called flow blocking in Barry (2008) and barrier jet in Smith (2019).

This dynamic barrier represents a mountain-like structure. Parameterisation scheme approximations assume that the dynamic barrier reduces the depth of the wind component perpendicular to the mountain (Figure 1). This means that a parcel of air will be displaced a shorter vertical distance (Figure 1b) compared to the normal case (Figure 1a), meaning a 'smaller' MW will form with a lower amplitude (H_{eff} in Equations 2 and 3 show this). If the blocking layer is at maximum depth (up to ridge height—Figure 1c) then the parameterisation scheme assumes no MWs will form. Now that the parcel of air was not displaced in Figure 1c, there should not form any MWs. This approach seems correct, but incorrectly assumes the width of the blocking layer is infinite.

The width of the blocking layer will depend on the barrier and meteorological conditions in question. The

width of blocking layers has been observed in many parts of the world, for example; 50 km in British Columbia (Overland & Bond, 1995), 80 km in South Africa (Geldenhuys et al., 2019), 81 km in the Gulf of Mexico (Luna-Nino & Cavazos, 2017) and 1–200 km in Alaska (Loescher et al., 2006). The width of the blocking jet can be anything from a few kilometres to a few hundred kilometres. This means the blocking layer width is within the same to 1 order of magnitude higher than the mountain width, but not infinitely wide. The model approaches discussed in this note focus on the direct vicinity of the mountain and fail to capture the characteristics of the larger system. It is the characteristics of the larger system that are relevant for the excitation of MWs.

3 | CONSIDERATIONS OF THE BLOCKING LAYER INFLUENCE ON DETERMINING MODEL GW DRAG

The blocking layer is known to be a narrow-sloping layer (Bell & Bossart, 1988; Geldenhuys et al., 2019; Neiman et al., 2010; Parish, 1982) as long as no upwind topography exists in the close vicinity. The dynamic barrier will have a maximum depth at the mountain face and will slope in the upwind direction (Figure 2). This means that an air parcel approaching the sloping barrier will either help build the blocking jet outwards or will be forced to rise above this 'mountain-like' structure. As early as Bell and Bossart (1988), it was suggested that the air parcel will rise above the sloping blocking layer (Figure 3). The air parcels passing over the dynamic barrier will be forced to rise from the surface to mountain height. The displacement height and the required work is the same as in the traditional MW case (Figure 1a). At the mountain top, the air parcels in Figure 2 will not be at equilibrium altitude and will fall to the lee side, forming an MW. The MW forming during blocking conditions will have an amplitude comparable to the case without a blocking layer, and should not be reduced as Equations 2 and 3 suggest.

It should be kept in mind that although the vertical displacement remains the same in the two cases (no blocking, Figure 1a, and realistic blocking layer, Figure 2), the GW field will differ. Multiple reasons are the cause of this. First, the width of the mountain has changed from a narrow ridge (barrier) to a broad barrier (as the blocking layer adds to the width of the barrier). Second, the blocking jet can produce its own MWs. The blocking jet blows parallel to the main ridge but perpendicular to the side ridges leading up to the main ridge. These have been observed to excite MWs and can cause different GWs to interfere; forming a complex pattern (Van der Mescht & Geldenhuys, 2019). The blocking air can also spill over the mountain forming an MW or a hydraulic jump (Geldenhuys et al., 2019).

The width of the barrier (mountain + dynamic barrier) will affect the GW field. In the blocking case, the horizontal wavelength of the GW will be longer since the displacement starts further upwind (Figure 2). A longer horizontal wavelength will reduce the GW momentum flux, but not nearly as much as the temperature amplitude. The effect of the temperature dominates in the model parameterisation scheme as the GW momentum flux can be brought to zero for a full blocking layer (when the temperature amplitude is 0 K). A longer horizontal wavelength can only reduce the GW momentum flux slightly (compared to zero GW momentum flux for an amplitude of 0 K). The fact that H_{eff} is squared in Equation 2 shows that the displacement height (directly proportional to the amplitude) affects the GW momentum flux exponentially in the model. Hence, it can be said that an incorrect horizontal wavelength is not nearly as bad as an incorrect temperature amplitude.

A blocking jet blowing parallel to the main ridge form ideal conditions for short horizontal scale MWs. The strong wind in a stable environment will blow over all the side ridges running up to the main ridge and has been linked with short-wavelength GWs producing severe turbulence (Van der Mescht & Geldenhuys, 2019).

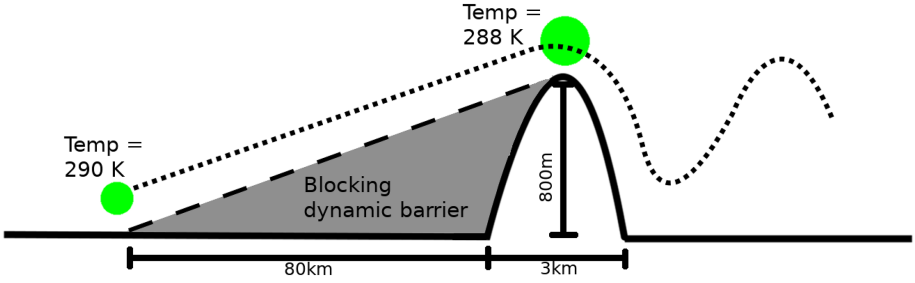

FIGURE 2 Airflow as expected in the vicinity of a blocking region. The blocking layer (shaded) is complete and extended up to ridge height while taking the form of a sloping dynamic barrier. Green circles indicate an air parcel being uplifted and the dotted line indicates wind flow projected perpendicular to the ridge. The figure is not to scale

Models using an anisotropy parameterisation scheme with a high-resolution orographic field can theoretically account for this.

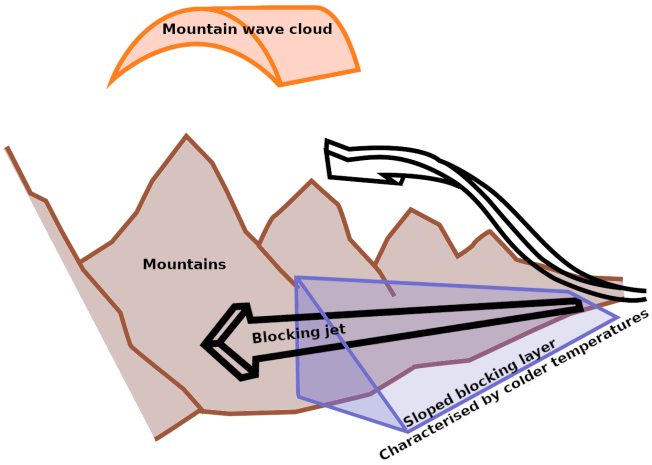

FIGURE 3 Adapted from Bell and Bossart (1988), who first suggested that the airflow will flow over the sloping blocking region. The incoming stable flow is deflected by the mountains to produce a blocking jet. The blocking region is known to be more stable, with a colder temperature and higher pressure. This region is indicated by the blue sloping dynamic barrier. Note the winds upwind of the blocking layer ascend the dynamic barrier as well as the mountains. The mountain wave cloud is not present in the original drawing, but was added here to show that the wind flowing over the barrier can induce GWs

A second mechanism in which a blocking layer can directly produce MWs is by air spilling downwind. Once the blocking layer reaches the altitude of the mountain ridge the blocking layer will continuously weaken by air spilling to the lee side. The spilt cold blocking air will accelerate down the lee slope and can adjust forming a hydraulic jump. The air rushing down the lee side has many implications (e.g., displacing cold pools, Lareau & Horel, 2014), but the important one here is the hydraulic jump that can form a propagating GW. The top of the blocking layer is characterised by a transitional Froude number (≈ 1). Such a Froude number has long been linked with producing waves in the lee of mountains (Figure 4). Such a mechanism has been observed from katabatic winds in Antarctica (Vignon et al., 2020; Watanabe et al., 2006; Yu & Cai, 2006) and in the blocking regime in South Africa (Geldenhuys et al., 2019).

Figure 5 from an idealised modelling study is good evidence of GWs originating from air spilling downwind. Note how the potential temperature lines indicate no upward displacement of isolines directly upwind of the barrier. This most likely indicates a blocking layer, inhibiting the air to be displaced in the normal manner. Also note the GW structure directly downwind of the barrier similar to what Figure 2 suggests. The GW structure is visible up to 8 km in Figure 5, highlighting the importance of this mechanism.

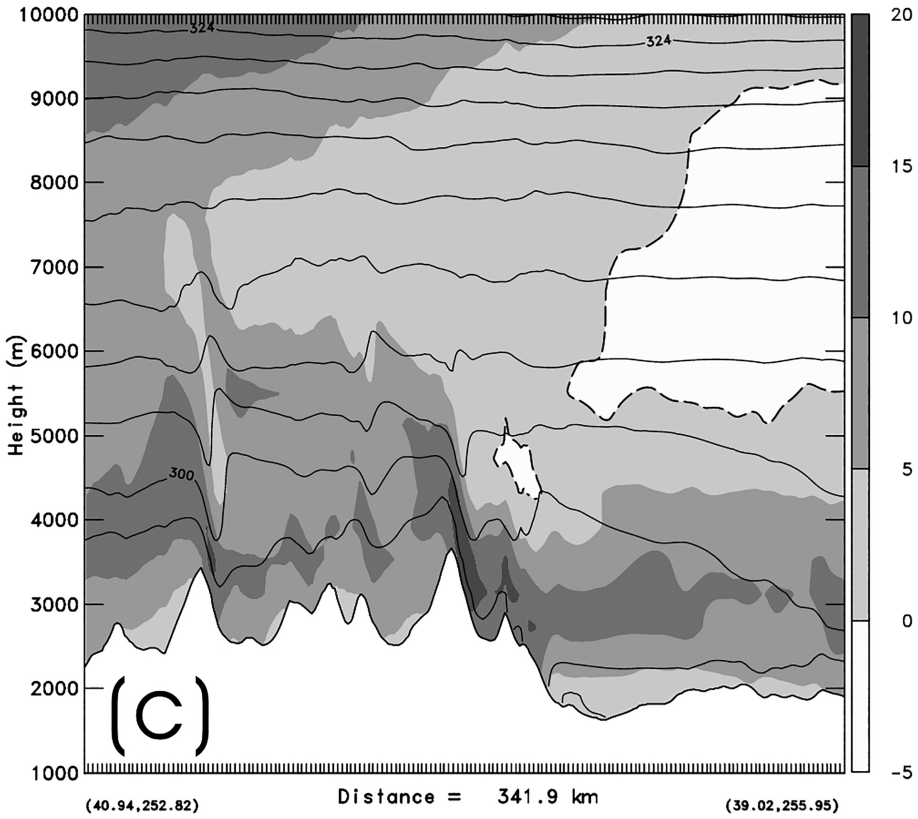

FIGURE 4 Fig. 9c from Kim and Doyle (2005) show an idealised modelling study over the Rockies. The wind blows from left to right in this plot. The grey shading shows zonal wind and the contour lines indicate potential temperature. Note the lack of vertical displacement upwind of the first and second ridge from the left, yet GWs are observed above them

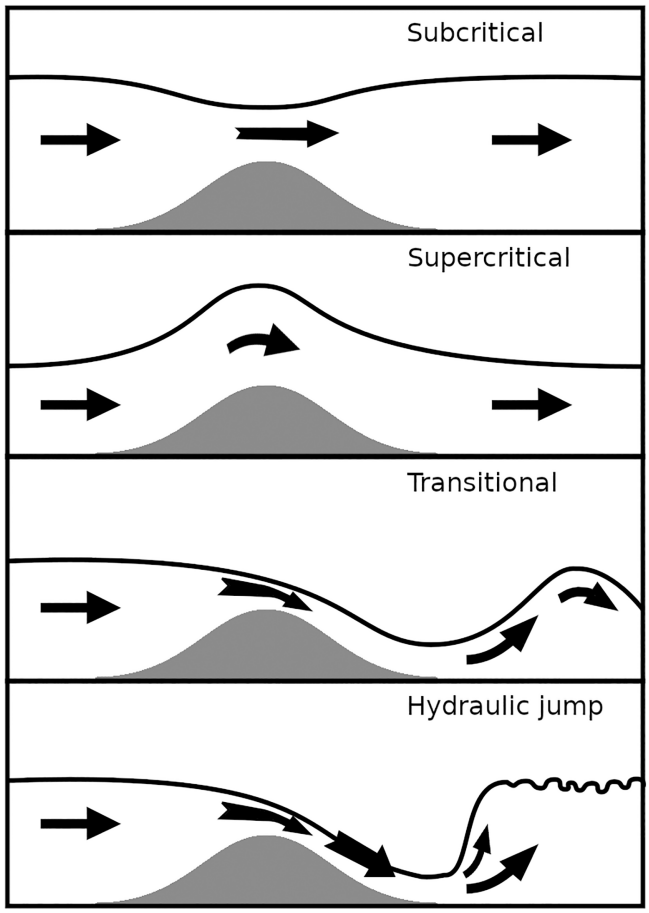

FIGURE 5 Flow over mountainous terrain with a subcritical, supercritical and transitional Froude number. The hydraulic jump will also take place during transitional flow. Adapted from Bradbury (1991)

Blocking creates a broad barrier that can produce GWs via alternative methods. Trüb and Davies (1995) provide a good overview of GWs that forms over a broad ridge (classified as having a halfwidth of up to a few hundred kilometres) for wind flow of differing Rossby numbers. Geldenhuys et al. (2021) introduces a new mechanism where a broad ridge (halfwidth $\approx$ 1500 km) pushes the tropospheric jet out of geostrophic balance as an indirect source for GWs. Depending on the model resolution, some of these GWs may be resolved, but that would require the blocking layer and the ridge to be adequately resolved.

4 | CONCLUSION

This note sets out to provide an argument to spark a debate among the GW community. The argument state that in contrast with current GW parameterisation schemes, the GW drag in the vicinity of blocking should not be reduced. Current parameterisation schemes reduce the incoming flow (and the resultant GW drag) by assuming the blocking layer is a new surface stretching infinitely upwind (called the effective topography). For a long time literature has dictated that the blocking layer is indeed sloped with a finite width (Figure 3), yet the model parameterisation schemes still ignore this. The main argument presented here states that the blocking layer forms a dynamic barrier that resembles a local extension of the mountain. Airflow impinging on a sloping blocking layer needs to join (and be deflected) this layer or be uplifted above this layer. The uplifted air resembles air being lifted by the mountain itself (Figures 2 and 3), hence the mountain just got broader. Parameterisations that take the grid points directly at the mountain and reduce the drag due to blocking will exclude the airflow from upwind (which is also uplifted and pass over the barrier).

Air being uplifted by a dynamic-mountain-barrier can result in several different GW formation patterns above and on the lee side. This note lists some of these patterns, but it is not the purpose of this note to review these patterns in detail. To illustrate one of the large shortcomings, let us assume an example of a complete blocking layer extending from surface to mountain peak. Current parameterisations assume no GW drag from this example (Figure 1c). However, stable heavier air will spill over the mountain and accelerate down the lee slope, surpassing equilibrium and forming a GW (Figure 2). This pattern is analogous to katabatic winds forming GWs off the coast of Antarctica. Similarly, parameterisations will represent GWs forming in a blocking layer with a proportional reduced GW drag; however, the origin of the air is much lower than the represented level (taken by the model as the top of the blocking layer). Meaning a GW will form with a larger amplitude and more drag. Literature indicates that broad ridges can result in indirect GWs by compressing the air above (Geldenhuys et al., 2021; Trüb & Davies, 1995). This is another GW production mechanism that models will miss.

All of the above patterns will excite GWs that propagate upwards and outwards depositing momentum as they break. Model parameterisation schemes do not account for this drag. I fully concede that in reality, the GW field with no blocking layer and with a blocking layer will look starkly different. How to represent this better remains an open question, but, reducing the GW drag in the vicinity of blocking to the current extent (to zero in some instances) might not be the best approximation.

An interesting experiment would be to undo these blocking limitations in the model and evaluate the impact. Naturally, the 'knob' present in all GW parameterisation

schemes might have to be turned down as the knob acts to compensate for the errors in the scheme. A high-resolution LES simulation will be another useful tool in analysing this. Overall it is my opinion that more work is required to improve the accuracy of the parameterised GW drag in the model, this consideration might contribute to this.

ACKNOWLEDGEMENT

The author would like to thank Manfred Ern for his comments that greatly improved this note.

CONFLICT OF INTEREST

The author declares no conflict of interest.

ORCID

Markus Geldenhuys https://orcid.org/0000-0001-6273-5633

REFERENCES

Bacmeister, J.T., Newman, P.A., Gary, B.L. & Chan, K.R. (1994) An algorithm for forecasting mountain wave-related turbulence in the stratosphere. *Weather and Forecasting*, 9, 241–253. https://doi.org/10.1175/1520-0434(1994)009<0241:AAFFMW>2.0.CO;2

Barry, R.G. (2008) *Mountian weather and climate*, 3rd edition. Cambridge: Cambridge University Press. https://doi.org/10.1017/CBO9780511754753

Bell, G.D. & Bossart, L.F. (1988) Appalachian cold-air damming. *Monthly Weather Review*, 116, 137–161. https://doi.org/10.1175/1520-0493(1988)116<0137:ACAD>2.0.CO;2

Berner, J., Achatz, U., Battè, L., Bengtsson, L., de la Camara, A., Christensen, H.M. et al. (2017) Stochastic parameterization: toward a new view of weather and climate models. *Bulletin of the American Meteorological Society*, 98, 565–588. https://doi.org/10.1175/BAMS-D-15-00268.1

Boeloeni, G., Kim, Y.-H., Borchert, S. & Achatz, U. (2021) Toward transient subgrid-scale gravity wave representation in atmospheric models. Part I: propagation model including non-dissipative wave–mean-flow interactions. *Journal of the Atmospheric Sciences*, 78, 1317–1338. https://doi.org/10.1175/JAS-D-20-0065.1

Bradbury, T., 1991. Wind shear and waves. *Sailplane and Gliding*. 178–182.

de la Camara, A., Lott, F., Valerian, J., Plougonven, R. & Hertzog, A. (2016) On the gravity wave forcing during the southern stratospheric final warming in LMDZ. *Journal of the Atmospheric Sciences*, 73, 3213–3226. https://doi.org/10.1175/JAS-D-15-0377.1

ECMWF, 2015. Part IV: dynamics and numerical procedures, IFS documentation CY41r1, IFS Documentation, ECMWF. https://doi.org/10.21957/p50qmwprw

Fritts, D.C. & Alexander, M.J. (2003) Gravity wave dynamics and effects in the middle atmosphere. *Reviews of Geophysics*, 41, 1003. https://doi.org/10.1029/2001RG000106

Fritts, D.C., Smith, R.B., Taylor, M.J., Doyle, J.D., Eckermann, S.D., Andreas, D. et al. (2016) The deep propagating gravity wave experiment (DEEPWAVE): an airborne and ground-based exploration of gravity wave propagation and effects from their sources throughout the lower and middle atmosphere. *Bulletin of the American Meteorological Society*, 97, 425–453. https://doi.org/10.1175/BAMS-D-14-00269.1

Garcia, R.R., Smith, A.K., Kinnison, D.E., de la Camara, A. & Murphy, D.J. (2017) Modification of the gravity wave parameterization in the whole atmosphere community climate model: motivation and results. *Journal of the Atmospheric Sciences*, 74, 275–291. https://doi.org/10.1175/JAS-D-16-0104.1

Geldenhuys, M., Dyson, L.L. & van der Mescht, D. (2019) Blocking, gap flow and mountain wave interaction along the coastal escarpment of South Africa. *Theoretical and Applied Climatology*, 139, 1291–1303. https://doi.org/10.1007/s00704-019-03030-4

Geldenhuys, M., Preusse, P., Krisch, I., Zülicke, C., Ungermann, J., Ern, M. et al. (2021) Orographically induced spontaneous imbalance within the jet causing a large-scale gravity wave event. *Atmospheric Chemistry and Physics*, 21, 10393–10412. https://doi.org/10.5194/acp-21-10393-2021

Kim, Y.-J. & Arakawa, A. (1995) Improvement of orographic gravity wave parameterization using a mesoscale gravity wave model. *Journal of the Atmospheric Sciences*, 52, 11875–11902. https://doi.org/10.1175/1520-0469(1995)052<1875:IOOGWP>2.0.CO;2

Kim, Y.-H., Boeloeni, G., Borchert, S., Chun, H. & Achatz, U. (2021) Toward transient subgrid-scale gravity wave representation in atmospheric models. Part II: wave intermittency simulated with convective sources. *Journal of the Atmospheric Sciences*, 78, 1339–1357. https://doi.org/10.1175/JAS-D-20-0066.1

Kim, Y.-J. & Doyle, J.D. (2005) Extension of an orographic-drag parameterization scheme to incorporate orographic anisotropy and flow blocking. *Quarterly Journal of the Royal Meteorological Society*, 131, 1893–1921. https://doi.org/10.1256/qj.04.160

Lang, S.T., Dawson, A., Diamantakis, M., Dueben, P., Hatfield, S., Leutbecher, M. et al. (2021) More accuracy with less precision. *Quarterly Journal of the Royal Meteorological Society*, 147, 4358–4370. https://doi.org/10.1002/qj.4181

Lareau, N.P. & Horel, J.D. (2014) Dynamically induced displacements of a persistent cold-air Pool. *Boundary-Layer Meteorology*, 154, 291–316. https://doi.org/10.1007/s10546-014-9968-5

Loescher, K.A., Young, G.S., Colle, B.A. & Winstead, N.S. (2006) Climatology of barrier jets along the Alaskan coast. Part I: spatial and temporal distributions. *Monthly Weather Review*, 134, 437–453. https://doi.org/10.1175/MWR3037.1

Lott, F., Guez, L. & Maury, P. (2012) A stochastic parameterization of non-orographic gravity waves: formalism and impact on the equatorial stratosphere. *Geophysical Research Letters*, 39, L06807. https://doi.org/10.1029/2012GL051001

Lott, F. & Miller, M.J. (1997) A new subgrid scale orographic drag parameterization: its formulation and testing. *Quarterly Journal of the Royal Meteorological Society*, 123, 101–127.

Luna-Nino, R. & Cavazos, T. (2017) Formation of a coastal barrier jet in the Gulf of Mexico due to the interaction of cold fronts with the Sierra Madre oriental mountain range. *Quarterly Journal of the Royal Meteorological Society*, 144, 115–128. https://doi.org/10.1002/qj.3188

McLandress, C., Shepherd, T.G., Saroja, P. & Beagley, S.R. (2012) Is missing orographic gravity wave drag near 60 degrees S the cause of the stratospheric zonal wind biases in chemistry climate models? *Journal of the Atmospheric Sciences*, 69, 802–818. https://doi.org/10.1175/JAS-D-11-0159.1

Neiman, P., Sukovich, E., Ralph, F. & Hughes, M. (2010) A seven-year wind profiler-based climatology of the windward barrier jet along California's northern Sierra Nevada. *Monthly Weather Review*, 138, 1206–1233. https://doi.org/10.1175/2009MWR3170.1

Overland, J. & Bond, N. (1995) Observations and scale analysis of coastal wind jets. *Monthly Weather Review*, 123, 2934–2941. https://doi.org/10.1175/1520-0493(1995)123<2934:OASAOC>2.0.CO;2

Parish, T.R. (1982) Barrier winds along the Sierra Nevada Mountains. *Journal of Applied Meteorology and Climatology*, 1962-1982(21), 925–930.

Pierrehumbert, R.T., 1986. An essay on the parameterization of orographic gravity wave drag, Seminar/workshop on observation, theory and modelling of orographic effects. Seminar: 15–19 September 1986. ECMWF, Shinfield Park, Reading, MA, pp. 251–282.

Plougonven, R., de la Camara, A., Hertzog, A. & Lott, F. (2020) How does knowledge of atmospheric gravity waves guide their parametrizations? *Quarterly Journal of the Royal Meteorological Society*, 146, 1529–1543. https://doi.org/10.1002/qj.3732

Polichtchouk, I., Shepherd, T.G. & Byrne, N.J. (2018) Impact of parametrized nonorographic gravity wave drag on stratosphere-troposphere coupling in the northern and southern hemispheres. *Geophysical Research Letters*, 45, 8612–8618. https://doi.org/10.1029/2018GL078981

Rapp, M., Kaifler, B., Dörnbrack, A., Gisinger, S., Mixa, T., Reichert, R. et al. (2021) SOUTHTRAC-GW: an airborne field campaign to explore gravity wave dynamics at the world's strongest hotspot. *Bulletin of the American Meteorological Society*, 102, E871–E893. https://doi.org/10.1175/BAMS-D-20-0034.1

Sandu, I., Bechtold, P., Beljaars, A., Bozzo, A., Pithan, F., Shepherd, T.G. et al. (2016) Impacts of parameterized orographic drag on the northern hemisphere winter circulation. *Journal of Advances in Modeling Earth Systems*, 8, 196–211. https://doi.org/10.1002/2015MS000564

Sato, K. & Hirano, S. (2019) The climatology of the Brewer-Dobson circulation and the contribution of gravity waves. *Atmospheric Chemistry and Physics*, 19, 4517–4539. https://doi.org/10.5194/acp-19-4517-2019

Serafin, S., Rotach, M.W., Arpagaus, M., Colfescu, I., Cuxart, J., De Wekker, S.F.J. et al. (2020) *Multi-scale transport and exchange processes in the atmosphere over mountains*, 1st edition. Innsbruck, Austria: Innsbruck University Press. https://doi.org/10.15203/99106-003-1

Smith, R.B. (2019) 100 years of Progress on mountain meteorology research. *Meteorological Monographs*, 59, 20. https://doi.org/10.1175/AMSMONOGRAPHS-D-18-0022.1

Trüb, J. & Davies, H.C. (1995) Flow over a mesoscale ridge: pathways to regime transition. *Tellus A: Dynamic Meteorology and Oceanography*, 47, 502–524. https://doi.org/10.3402/tellusa.v47i4.11542

Van der Mescht, D. & Geldenhuys, M. (2019) Observations of mountain waves with interference generated by coastal mountains in South Africa. *Meteorological Applications*, 26, 409–415. https://doi.org/10.1002/met.1771

Van Niekerk, A. & Vosper, S.B. (2021) Towards a more "scale-aware" orographic gravity wave drag parametrization: description and initial testing. *Quarterly Journal of the Royal Meteorological Society*, 147, 3243–3262. https://doi.org/10.1002/qj.4126

Vignon, E., Picard, G., Durán-Alarcón, C., Alexander, S.P., Gallée, H. & Berne, A. (2020) Gravity wave excitation during the coastal transition of an extreme katabatic flow in Antarctica. *Journal of the Atmospheric Sciences*, 77, 1295–1312. https://doi.org/10.1175/JAS-D-19-0264.1

Watanabe, S., Sato, K. & Takahashi, M. (2006) A general circulation model study of the orographic gravity waves over Antarctica excited by katabatic winds. *Journal of Geophysical Research*, 111, D18104. https://doi.org/10.1029/2005JD006851

Xie, J., Zhang, M., Xie, Z., Liu, H., Chai, Z., He, J. et al. (2019) An orographic-drag Parametrization scheme including orographic anisotropy for all flow directions. *Journal of Advances in Modeling Earth Systems*, 12, e2019MS001921. https://doi.org/10.1029/2019MS001921

Yu, Y. & Cai, X. (2006) Structure and dynamics of katabatic flow jumps: idealised simulations. *Boundary-Layer Meteorology*, 118, 527–555. https://doi.org/10.1007/s10546-005-6433-5

How to cite this article: Geldenhuys, M. (2022). On gravity wave parameterisation in vicinity of low-level blocking. *Atmospheric Science Letters*, *23*(6), e1084. https://doi.org/10.1002/asl.1084